X-ray microtomographic characterisation of pore evolution during homogenisation and rolling of Al–6Mg

Y. M. Youssef[1], A. Chaijaruwanich[1], R. W. Hamilton[1], H. Nagaumi[2], R. J. Dashwood[1] and P. D. Lee*[1]

The effect of homogenisation heat treatment and subsequent hot rolling on the evolution of porosity in a direct chill cast Al–6Mg (wt-%) alloy was studied. Porosity was quantified using conventional 2D optical metallography and X-ray microtomography (XMT) which allowed 3D imaging. Metallographic observations show an increase in maximum pore length during heat treatment and at the centre line during rolling. These observations together with the high temperatures might suggest a classical interpore Ostwald ripening mechanism is operative. However, XMT revealed that the pores have a highly tortuous shape, which when sectioned metallographically is not apparent and can lead to misinterpretation. X-ray microtomography observations proved that these tortuous 3D shapes spheroidised during homogenisation owing to localised coarsening of high curvatures within the complex, branching structure of each pore, termed intrapore coarsening. Accelerated centreline intrapore coarsening was observed during the initial rolling passes when relatively low reduction ratios were used. Finite element modelling was used to demonstrate that under the geometric rolling conditions employed the central region of the billet experienced a tensile rather than a compressive hydrostatic stress. This combined with deformation enhanced diffusion is proposed as the reason for the accelerated intrapore spheroidisation. X-ray microtomography was critical to revealing the true 3D pore shape and the mechanisms of pore coarsening, which could have been misinterpreted if only 2D metallography was used.

Keywords: Porosity, Homogenisation, Rolling, X-ray tomography, Al–6Mg alloy

Introduction

The microstructure resulting from most casting processes may contain pores formed from the combined effect of the partitioning of insoluble gases (hydrogen for aluminium) and incomplete feeding of the volumetric change upon solidification.[1–3] The percentage and size of the porosity increases with increasing initial hydrogen content.[4–6] Other factors influencing porosity formation include:

(i) the cause of nucleation, for example, oxides[7]
(ii) alloy composition[4,8]
(iii) solidification conditions.[9,2]

In most products produced from direct chill (DC) cast aluminium alloys, subsequent thermomechanical processing (TMP) is applied and the pores are assumed to be closed (termed healed). However, in some products it was observed that pore closure was incomplete. If porosity remains, it has been shown to be detrimental to the final mechanical properties, especially fatigue life.[10–14] The present study will investigate pore closure during subsequent processing, specifically homogenisation and hot rolling. Homogenisation is used to reduce microsegregation and hot rolling (or other thermomechanical processing, such as forging or extrusion) is used to control mechanical properties through grain size refinement and defect removal.

Homogenisation employs long holding periods at high temperature to accelerate solid state diffusion and consequently reduce microsegregation. Traditionally, it has been assumed that porosity is eliminated during TMP. For this reason the evolution of pore morphology and size during homogenisation and subsequent thermomechanical processing is still not fully understood. There have been only a few prior studies on the influence of homogenisation upon porosity in aluminium alloys.[15–18] While these studies showed that porosity increases during homogenisation, the results

[1]Department of Materials, Imperial College London, Exhibition Road SW7 2AZ, UK
[2]Nippon Light Metal Co. Ltd, Nikkei Research & Development Centre, 1-34-1 Kambara, Japan

*Corresponding author, email p.d.lee@imperial.ac.uk

Published by Maney on behalf of the Institute
Received 15 February 2006; accepted 19 April 2006
DOI 10.1179/174328406X114171

are not consistent and hence there is limited quantification of the effect.

The effect of hot and cold rolling on porosity in aluminium was studied experimentally by Talbot and Granger[16] who found that pores were flattened during hot rolling with a total of 90% reduction. Although no computational investigations were found pertaining to aluminium rolling, Wang *et al.*[19] studied pore closure during the hot rolling of steels. They suggested that the rate of pore closure was a function of reduction ratio, concluding (based on finite element simulations) that there is a minimum hydrostatic pressure required for pore closure and that the holding time at such pressure determines the degree of surface welding of the pores. Industry uses a range of reductions, therefore, an understanding of the mechanisms governing pore growth/closure during hot rolling is required.

The aim of the present study is to provide a quantitative investigation of the effect of homogenisation and rolling on the morphology and size of porosity in a DC cast Al–6Mg alloy. Laboratory scale hot rolling experiments were conducted simulating an industrial rolling schedule. Characterisation via both conventional metallography and X-ray microtomography (XMT) was performed, allowing both 2D and 3D quantification of porosity. 3D characterisation proved to be critical for determining the mechanism governing pore evolution. This confirms the hypothesis of Anson and Gruzleski[20] that observations based on 2D sectioning could be highly misleading. Metallographic observations, in isolation, suggest classical interpore Ostwald ripening. However, looking at the evolution of the pore in 3D demonstrates that local ripening of individual pores (intrapore) causes their initially highly tortuous morphology to spheroidise.

Experimental

Direct chill cast ingots with a cross-section of 250×400 mm and nominal composition Al–6Mg (*see* Table 1) were produced by NLM (Nippon Light Metals Co. Ltd, Kambara, Japan). Half the ingot was homogenised at 530°C for 10 h. This temperature was reached using a ramp rate of 50°C h^{-1} ($\sim$0·0139°C s^{-1}), followed by furnace cooling at 35°C h^{-1} ($\sim$0·0097°C s^{-1}). Rolling specimens were sectioned from the central region (80–100 mm from the chill surface) of the ingot, where the percentage porosity was at a maximum.[21] Rolling trials were performed using a four high rolling mill consisting of 125 mm diameter back-up rolls with 38 mm diameter work rolls. The plates (initially 20 mm thick by 100 mm wide and 90 mm long) were preheated to 400°C before rolling at 23 rev min^{-1}. A constant per pass reduction of 0·6 mm was used yielding a 3% reduction for the first pass increasing to 5·5% for the sixteenth pass. The final thickness after rolling was 10·4 mm. The specimen thickness was measured between each pass before reheating to 400°C. At passes 4, 8, 12 and 16, the specimen was quenched and 30 mm samples were cut from the end for metallographic examination.

Table 1 Nominal composition of Al–6Mg alloy used in present study, wt-%

Mg	Si	Fe	Cu	Ti	Mn	Cr	Al
6·16	0·02	0·02	<0·01	<0·01	<0·01	<0·01	Bal.

Additional homogenisation conditions were obtained using $20 \times 20 \times 50$ mm specimens in a laboratory furnace under the same ramp/cooling conditions as above. Additional conditions studied were: F– as cast; H1 – 1 h at 530°C; H100 – 100 h. The standard 10 h treatment is denoted as H10.

For metallographic samples, pore size (equivalent diameter and maximum Feret length) was quantified using a Neophot 21 optical microscope equipped with a KS400 (Zeiss KS 400, Imaging Associates Ltd, Oxon, UK) image analysis system. The total area examined per sample ranged between 80–102 mm^2, measuring between 30 and 70 pores (depending on the level of porosity) after features <30 μm equivalent diameter were discarded.

For the XMT examination, 2·5 mm diameter rods were machined from the as cast, industrially heat treated ingots and from specimens perpendicular to the rolling face. A 1 mm high region in the centre of each rod was scanned using a commercial XMT unit (Phoenix X-ray Systems &Services GmbH, Wunstorf, Germany) with a voltage of 80 kV and a current of 120 mA. Seven hundred and twenty images were captured on a detector of 1024×512 pixels over one revolution and then reconstructed with a voxel size of 3 μm. Image processing and porosity analysis were performed using VGStudio Max 1·2 (Volume Graphics GmbH, Heidelberg, Germany). A $3 \times 3 \times 3$ median filter was applied to reduce the noise. This threshold value was individually determined for each sample and then applied in a defect detection algorithm to quantify porosity. A minimum detectable pore size of 8 voxels (equivalent diameter of 7 μm) was used, measuring between 350 and 2000 pores in an area of $\sim$5 mm^3.

Results and discussion

Metallographic characterisation of pore evolution during homogenisation and rolling will be presented first followed by the XMT results.

Optical micrographs of typical pores in the as cast billet are shown in Fig. 1*a*, with typical changes in structure after 1 and 10 h homogenisation time shown in Fig. 1*b* and *c*. The pores are present as clusters. The cluster size does not appear to change significantly after homogenisation; however, the individual pore size increases.

The further evolution of pore morphology in the central portion of the plate during rolling is shown metallographically in Fig. 2. After 4 passes it is hard to determine what changes are occurring (Fig. 2*a* and *b*). However, after 12 passes (Fig. 2*c*) the pores become rounder and have a larger area (confirmed quantitatively below). By the sixteenth rolling pass (Fig. 2*d*) the pores have started to become flatter.

These results appear to show that the pores grow during homogenisation and the initial stages of rolling. Based on the evidence presented so far, the only mechanism which could be hypothesised as the driving force for this apparent growth is interpore coarsening. This seems feasible during homogenisation but is

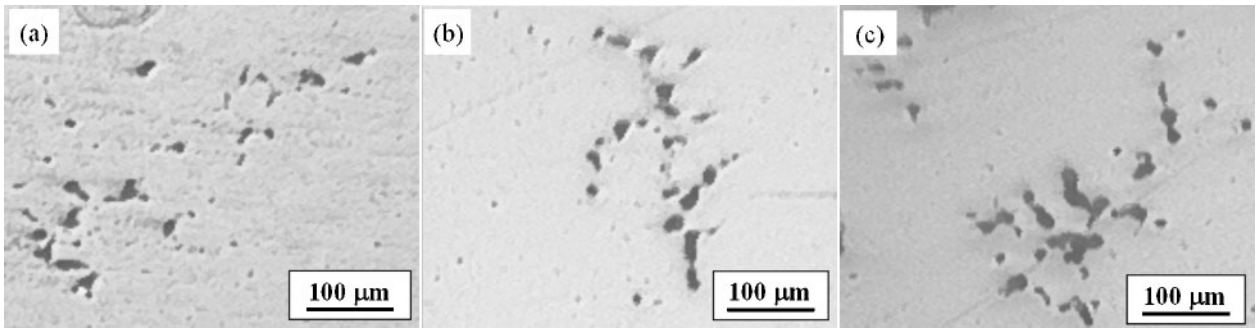

a F; *b* H1; *c* H10

1 Metallographically observed pore evolution during homogenisation of Al–6Mg

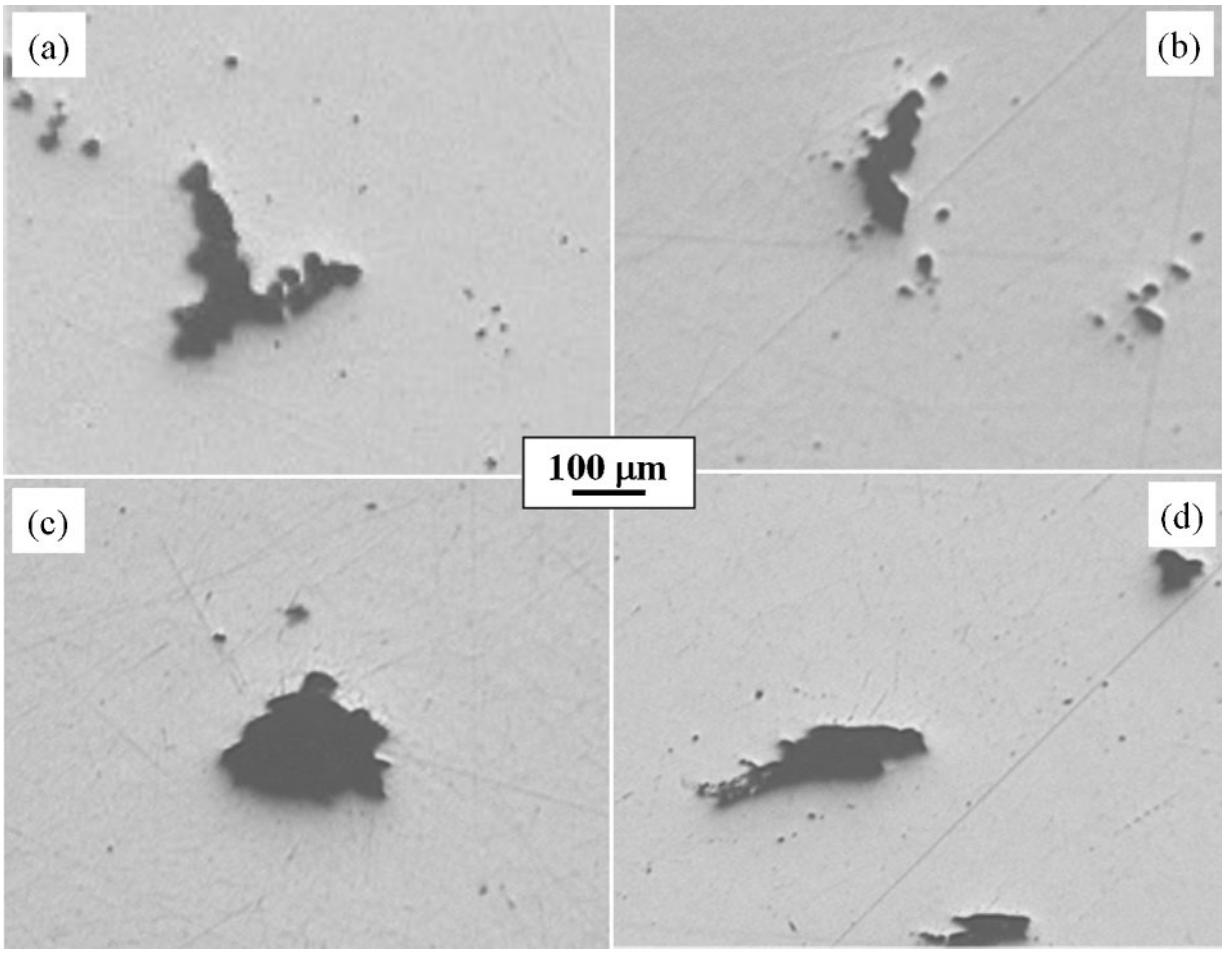

a 0; *b* 4; *c* 12; *d* 16

2 Metallographically observed pore evolution during rolling of Al–6Mg_H10 after pass

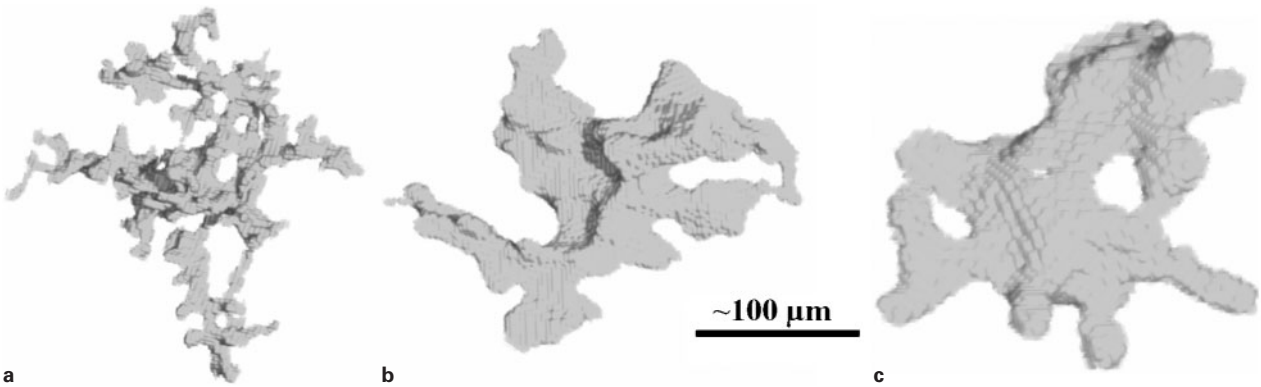

a F; *b* H10; *c* H100

3 X-ray microtomography observed pore evolution during homogenisation of Al–6Mg

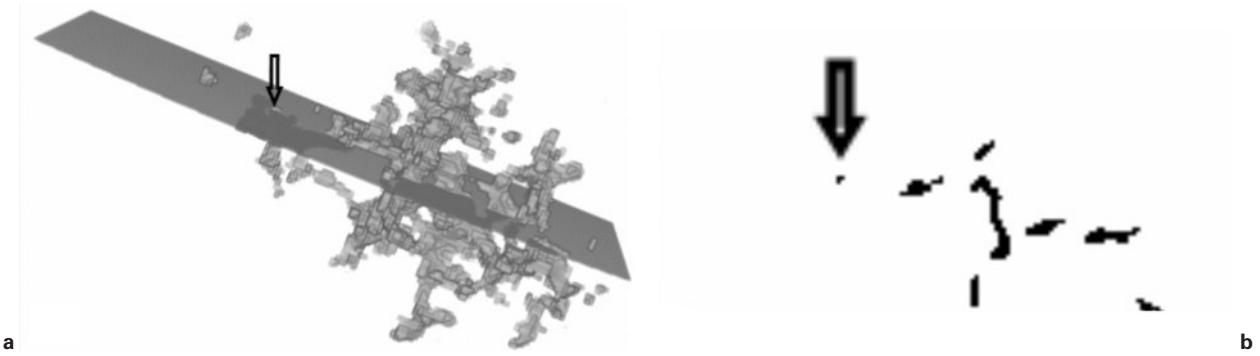

a b

4 Comparison of *a* 3D pore morphology with that observed on *b* 2D section

unlikely during rolling. Therefore, the same samples were examined using XMT.

The evolution of porosity during homogenisation as characterised via XMT is shown qualitatively in Fig. 3. Examining the as cast pore structure first, XMT illustrates that each cluster of small pores observed metallographically (Fig. 1*a*) was in fact a single, highly tortuous pore (Fig. 3*a*). Although pores are spherical when they nucleate, they are constrained within the interdendritic regions of the solidifying semisolid, wicking into the regions of liquid between the dendrites/grains. The extent of the misinterpretation possible in pore size and shape is illustrated in Fig. 4. Measurements of the 2D cut of this complex shaped pore would give incorrect values for both the number and size of porosity.

During homogenisation, the regions of high curvature in these tortuous networks tend to become smoother. After 10 h (Fig. 3*b*) the fine arms have thickened and shortened. After 100 h (Fig. 3*c*) the sharp radii have been smoothed and the pores have become more globular.

A similar effect is seen during rolling (Fig. 5). The pores initially are in the H10 state, with the as cast tortuousity having been reduced but not eliminated (Fig. 5*a*). As rolling proceeds the curvatures further

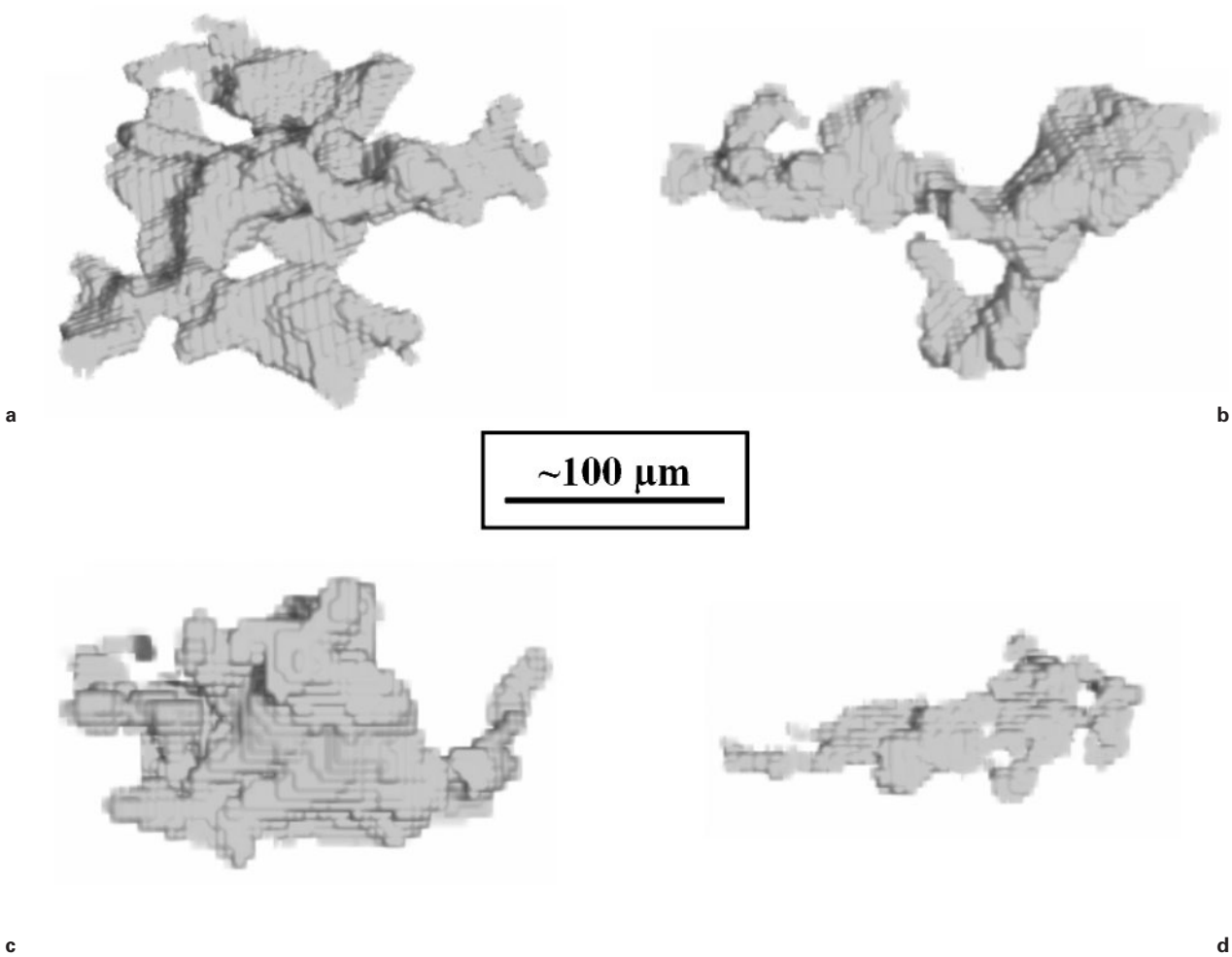

a b

c d

a 0; *b* 4; *c* 12; *d* 16

5 X-ray microtomography observed pore evolution during rolling of Al–6Mg_H10 after pass

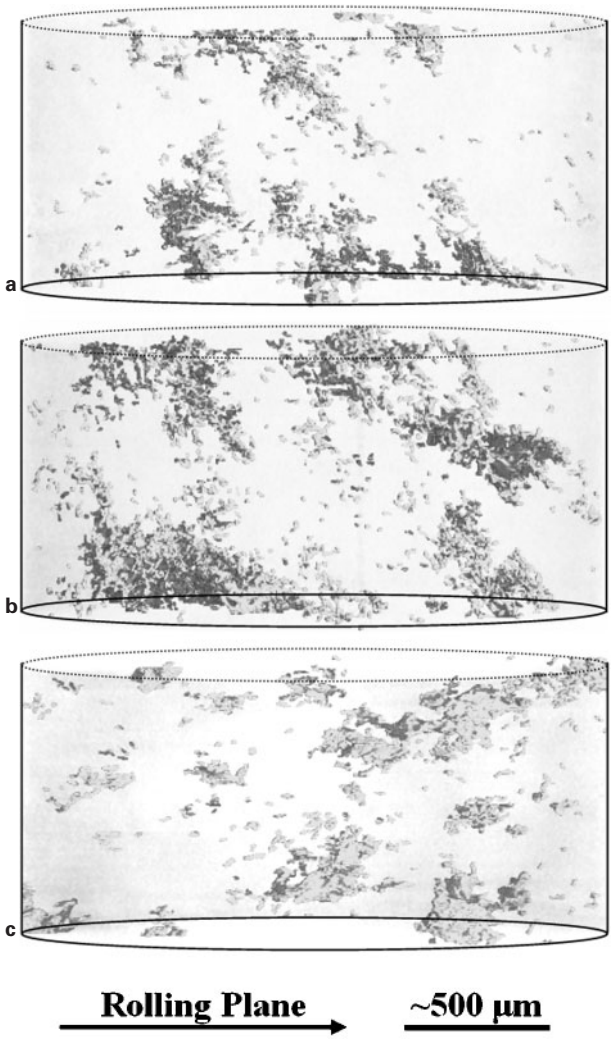

6 X-ray microtomography rendering of porosity in larger volume of Al–6Mg for *a* F, *b* H10 and *c* after 12 rolling passes

relax, branching is reduced, and spheroidisation occurs (Fig. 5*b* and *c*). If the authors compare the rate of spheroidisation during rolling with that during homogenisation, one might expect it to be less as the temperature is lower and the times shorter. However, comparing the extent of spheroidisation in Figs. 3 and 5, the overall effect of rolling is considerably larger than that observed during homogenisation. During the final stages of rolling (passes 12 to 16) the pores start to elongate (Fig. 5*c* and *d*) parallel to the rolling plane and compress in the normal direction.

Metallographic results suggested that classical interpore coarsening might be occurring. However the XMT results suggest another mechanism is operative, namely local coarsening of the high curvature regions of individual pores (intrapore coarsening). High temperature and long times are required for classical Ostwald ripening, neither of which are true during rolling. For intrapore coarsening, the distances are small since they are only the secondary dendrite arm spacings (on the order of 10 μm) and the diffusion will be enhanced by both surface effects and the vacancies generated during rolling.

Although only individual pores were used as examples, the XMT reconstructions of the whole specimen ($\sim$2 mm diameter $\times$ 1·5 mm) show that the effects are consistent over many scanned pores (Fig. 6). The degree of branching is reduced after homogenisation for 10 h (Fig. 6*b*) and after the subsequent twelve rolling passes the pores coarsened further and became elongated in the rolling plane (Fig. 6*c*).

Quantitative analysis of the metallographic (denoted by superscript '*M*') and tomographic (denoted by superscript '*X*') data further demonstrates the misinterpretation that could occur if these complex structures are only analysed in 2D. During rolling, the metallographic results suggest a steady increase in both the mean equivalent (circular) pore diameter D^{M}_{avg} (Fig. 7*a*) and the maximum Feret length F^{M}_{max} (Fig. 7*b*). Between passes 12 and 16 the overall size reduces slightly. The XMT data show that this is not the case and in fact show that the maximum equivalent (spherical) diameter D^{X}_{max} does not change significantly (Fig. 8). This indicates that the overall volume of each pore stays constant. However, the maximum dimension of the largest pore L^{X}_{max} reduces by $\sim$30%. This agrees with the qualitative observations (Fig. 5) that the pores are becoming more rounded.

Using the XMT data, a shape factor can be calculated from the ratio of the sum of the measured surface areas

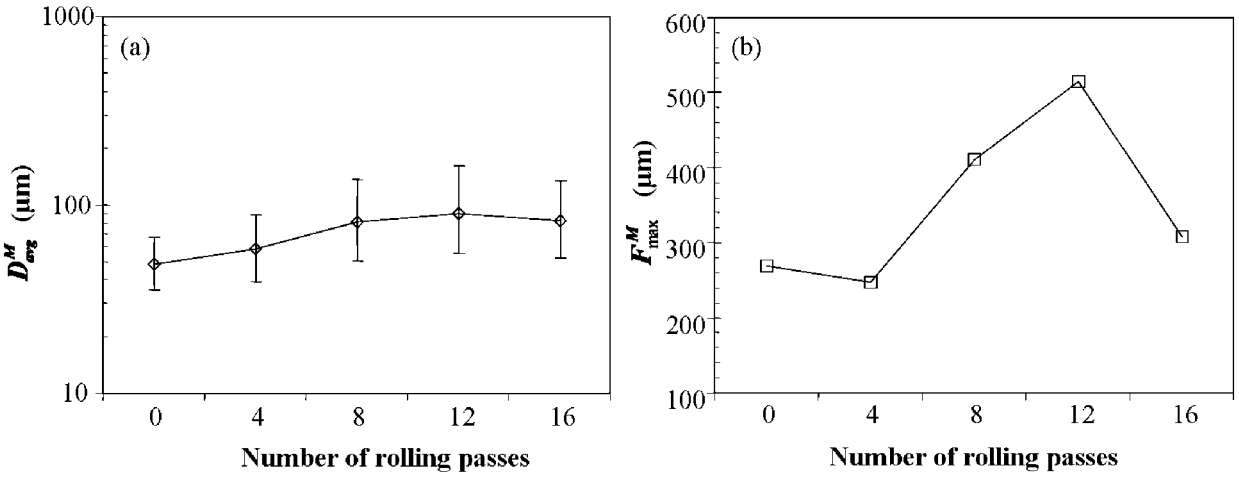

7 Metallographically quantified *a* mean equivalent pore diameter D^{M}_{avg} and *b* maximum Feret length F^{M}_{max} as function of number of rolling passes for Al–6Mg alloy after H10

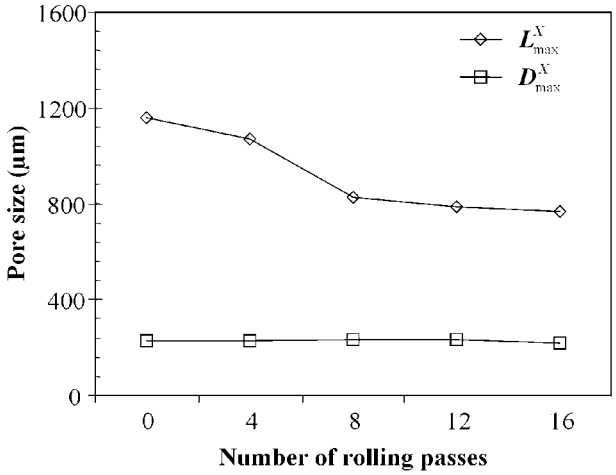

8 X-ray microtomography quantified maximum equivalent pore diameter D^X_{max} and maximum pore length L^X_{max} as function of number of rolling passes for Al–6Mg alloy after H10

over the sum of the surface areas of equivalent volume spheres (Fig. 9). The pore shape factor is equal to one for a spherical pore. This ratio decreased at every processing step from the as cast billet through homogenisation to hot rolling, illustrating that the pores are spheroidising. There is a small drop after 10 h homogenisation (from 7·3 to 6·8) followed by a sharp decrease during the initial four rolling passes (6·8 to 4·2). It is hypothesised that this coarsening occurs by surface diffusion reducing the regions of high curvature on the asperities of these tortuous pores, termed intrapore coarsening. Owing to the high temperature (530°C) and long time (10 h) associated with the homogenisation treatment one might expect this stage to result in the greatest level of coarsening. This is not the case. The most significant coarsening actually occurs in the earliest stages of rolling. To elucidate the reasons for this accelerated coarsening the stress state during rolling was modelled using Forge 2® (Transvalor SA Sophia Antipolis, France). Simulating the geometries used experimentally, which are geometrically similar to one set of typical industrial conditions, it can be seen that the deformation is concentrated in the surface layers and does not penetrate to the centreline of the plate

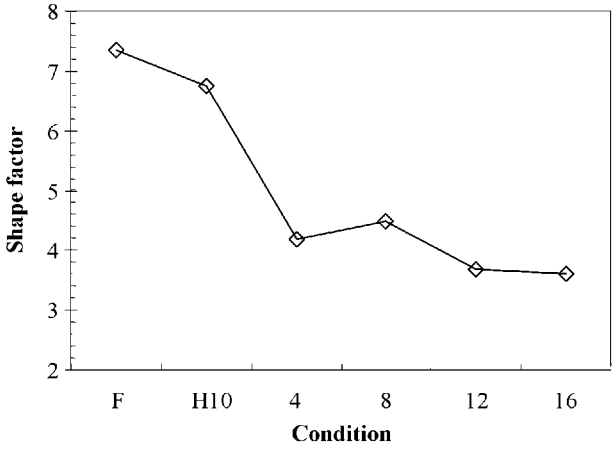

9 Shape factor evolution as function of homogenisation and number of rolling passes for Al–6Mg alloy (XMT): numbers indicate rolling passes

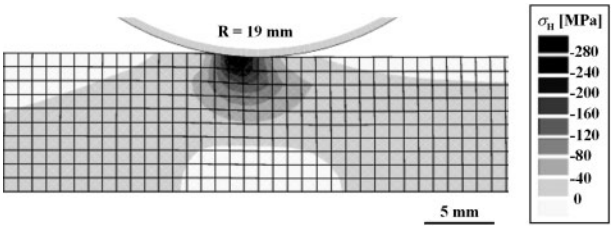

10 Hydrostatic stress σ_H distribution during plane strain rolling of 20 mm thick plate with roll radii *R* of 19 mm

(Fig. 10). Indeed at the centreline there is a tensile hydrostatic stress. This would explain the accelerated coarsening that took place. The tensile hydrostatic stress will prevent pore closure while increasing coarsening owing to deformation assisted vacancy diffusion. Previous work supports this hypothesis. Wang *et al.*[19] suggested that the magnitude and sign of the hydrostatic stress experienced was the critical parameter in determining pore closure.

Conclusions

A comparative study of pore evolution from an as cast billet, though homogenisation and 16 rolling passes was performed using metallographic and XMT characterisation. The metallographic results suggested that the pores were growing via a classical interpore Ostwald ripening mechanism. However, XMT revealed that the as cast pores had highly tortuous 3D morphologies which were not apparent from the metallographic sections. X-ray microtomography observations also showed that these tortuous 3D shapes spheroidised during homogenisation. It is hypothesised that surface diffusion leads to a localised reduction in curvature of the sharp asperities within the complex, branching structure of each pore, termed intrapore coarsening.

Accelerated centreline intrapore coarsening was observed during the initial rolling passes when relatively low reduction ratios were used. Finite element modelling was used to demonstrate that under the rolling conditions employed the central region of the billet experienced a tensile rather than a compressive hydrostatic stress. This combined with deformation enhanced diffusion is proposed as the reason for the accelerated intrapore spheroidisation.

Acknowledgements

The authors wish to acknowledge the support of the EPSRC (GR/T26344) and one of the authors (AC) would like to thank the Thai government for financial support. This contribution is based on a presentation at the International Workshop on 'Applications of X-ray tomography to study fracture and crack growth' held at Churchill College, Cambridge, UK in April 2005. The workshop was supported by Office of Naval Research Global under Department of the Navy Grant N00014-05-1-1043. The United States Government retains a royalty free licence throughout the world in all copyrightable material contained herein.

References

1. E. J. Whittenberger and F. N. Rhines: *J. Met.*, 1952, 409.
2. P. D. Lee and J. D. Hunt: *Acta Mater.*, 1997, **45**, 4155.

3. P. D. Lee, A. Chirazi and D. See: *J. Light Met.*, 2001, **1**, 15.
4. Q. T. Fang, P. N. Anyalebechi and D. A. Granger: in 'Light metals 1988', (ed. L. G. Boxall), 477; 1988, Phoenix, AZ, The Metallurgical Society.
5. G. Boudreault, A. M. Samuel, F. H. Samuel and H. W. Doty: Proc. 36th Ann. Conf. on 'Metallurgists', (ed. C. M. Bickert and R. I. L. Guthrie), 369; 1997, Sudbury, Ontario, CIM.
6. P. D. Lee, R. C. Atwood, R. J. Dashwood and H. Nagaumi: *Mater. Sci. Eng. A*, 2002, **328A**, 213.
7. J. Campbell: *Mater. Sci. Technol.*, 2006, **22**, 127.
8. X. G. Chen and S. Engler: *Metall*, 1991, **45**, 1225.
9. K. Tynelius, J. F. Major and D. Apelian: *AFS Trans.*, 1994, **101**, 401.
10. J. F. Major: *AFS Trans.*, 1998, **105**, 901.
11. Q. G. Wang, D. Apelian and D. A. Lados: *J. Light Met.*, 2001, **1**, 73.
12. J. Z. Yi, Y. X. Gao, P. D. Lee, H. M. Flower and T. C. Lindley: *Metall. Mater. Trans. A*, 2003, **34A**, 1879.
13. J. Fan, D. L. McDowell, M. F. Horstemeyer and K. Gall: *Eng. Fract. Mech.*, 2003, **70**, 1281.
14. Y. X. Gao, J. Z. Yi, P. D. Lee and T. C. Lindley: *Acta Mater.*, 2004, **52**, 5435.
15. M. F. Jordan, G. D. Denyer and A. N. Turner: *J. Inst. Met.*, 1962, **91**, 48.
16. D. E. J. Talbot and D. A. Granger: *J. Inst. Met.*, 1963, **92**, 290.
17. Y. G. Grishkovets, L. V. Budanova and D. A. Morgacheva: *Met. Sci. Heat Treat.*, 1984, **25**, 604.
18. P. N. Anyalebechi: Light Metals 1988, San Antonio, TX, USA, February 1988, TMS, 827.
19. A. Wang, P. F. Thomson and P. D. Hodgson: *J. Mater. Process. Technol.*, 1996, **60**, 95.
20. J. P. Anson and J. E. Gruzleski: *Mater. Charact.*, 1999, **43**, 319.
21. H. Nagaumi, K. Komatsu, M. Uematsu, N. Hagisawa and Y. Nishikawa: *Jpn Inst. Light Met.*, 1999, **6**, 13.